

AIR-WATER FLOW CHARACTERISTICS IN HYDRAULIC JUMP ON PEBBLED ROUGH BED

FARHAD BAHMANPOURI⁽¹⁾, CARLO GUALTIERI⁽²⁾ & HUBERT CHANSON⁽³⁾

⁽¹⁾ University of Napoli Federico II, Napoli, Italy (farhad.bahmanpouri@unina.it)

⁽²⁾ University of Napoli Federico II, Napoli, Italy (carlo.gualtieri@unina.it)

⁽³⁾ The University of Queensland, Brisbane, Australia (h.chanson@uq.edu.au)

ABSTRACT

The hydraulic jump is a sudden transition from a supercritical flow to a subcritical motion, characterised by strong turbulence, air entrainment and energy dissipation. A hydraulic jump results in strong interactions between turbulence, free-surface and air-water mixing. Past research on hydraulic jump with bed roughness focused on the identification of basic parameters including conjugate depth ratio, roller length and mean velocity. However, to date, only very few studies have addressed the air-water flow parameters. This paper aims to investigate the basic parameters of air-water flow in hydraulic jump on pebbled rough bed. The experiments were performed in a channel with partially-developed inflow conditions. The gravel materials, mixed natural river pebbles, were installed on the bed for the whole length of the flume. A phase-detection double-tip conductivity probe was used to measure the basic air-flow properties. The experiments were conducted for discharges ranging from 0.06 to 0.1 m³/s, corresponding to inflow Froude numbers Fr_1 between 1.7 and 2.84 and Reynolds number Re_1 from 170,000 to 220,000. Comparisons between rough and smooth bed data, as well as with the literature highlighted some distinctive effects of the non-uniform bed roughness. The results on rough pebble bed showed a shorter roller length and higher magnitudes of air-flow properties including void fraction and bubble count rate than those on smooth bed, especially in the region close to the jump toe.

Keywords: Hydraulic jump, Air-Water Flow, Pebbled Rough Bed, Physical Modelling

1 INTRODUCTION

A hydraulic jump is a transition from supercritical to subcritical flow, characterised by a strong dissipative mechanism and a region of rapidly varied flow (Chanson 2004). The flow turbulence in hydraulic jump is three-dimensional and extremely complex, remaining a challenge to engineers, scientists and researchers (Rajaratnam 1967; Chanson 2009). The first description of hydraulic jump by Leonardo da Vinci may be traced back to the 16th Century (Montes 1998). On smooth bed, early laboratory studies of air-water flows in hydraulic jumps were conducted by Rao and Kobus (1971) and Wood (1991). Gualtieri and Chanson (2007) investigated the effect of inflow Froude number upon the hydraulic jump on smooth bed. Chanson (2011) studied the hydraulic jump properties in terms of free-surface profile, fluctuation magnitude and frequencies. An empirical law of self-similar free-surface profile was proposed by Chanson (2011) within the roller length. Wang (2014) and Wang and Chanson (2015, 2016) comprehensively reported the basic parameters and air-entrainment properties of hydraulic jump on smooth for different inflow conditions. Valero et al. (2018) reviewed the available experimental datasets on the hydraulic jump to identify the main parameters relevant to the validation of numerical studies on the hydraulic jump. Hughes and Flack (1984) measured hydraulic jump characteristics over several artificially roughened test beds in a horizontal rectangular flume with smooth side walls. Ead and Rajaratnam (2002) evaluated the hydraulic jumps on corrugated beds. Their experiments were performed for a range of Froude numbers from 4 to 10. Carollo et al. (2007) investigated the conjugate depth ratio and roller length for hydraulic jump on rough gravel bed with 5 different bed material sizes. Pagliara et al. (2011) analyzed the hydraulic jump in homogeneous and non-homogeneous rough bed configurations including crushed angular rocks and hemispherical boulders. Felder and Chanson (2016,2018) studied the air-water flows in hydraulic jumps with channel bed roughness including two different rubber mat configurations of macro-roughness.

This paper presents the findings of an experimental study of a hydraulic jump on pebbled rough bed, with a focus on the air-water flow properties. Basic flow properties in both shear region and recirculation zone were investigated and compared to those on smooth bed. The results are discussed in relation to existing literature on air-water flows in hydraulic jumps.

2 EXPERIMENTAL SETUP. CHANNEL AND INSTRUMENTATION

The experiments were conducted in the hydraulics laboratory of the University of Queensland, in a flume used previously (Wang 2014; Wang and Chanson 2015; Felder and Chanson 2016,2018). The rectangular test section was 3.2 m long, 0.5 m wide and 0.41 m high, consisting of a horizontal high-density polyethylene (HDPE) bed and glass sidewalls. A constant flow rate was supplied from an upstream head tank through a vertical sluice gate equipped with a semi-circular edge ($\varnothing = 0.3$ m) to prevent flow contraction downstream of the upstream gate (Figure 1). In the present experiments, the jump toe position was located at $x_1 = 1$ m downstream of the sluice gate, for all flow conditions. The jump toe positions were controlled by a downstream overshoot gate. The water was fed into the head tank from a constant head reservoir. The flow rate was measured with a Venturi meter mounted in the supply pipe with an accuracy of $\pm 2\%$. LED light projectors were used for recording videos with high speed video cameras. Table 1 summarises the experimental conditions of the present study. Herein, the experiments were conducted for a range of discharges $0.012 \leq Q \leq 0.106$ m³/s, corresponding to an inflow Froude number Fr_1 in the range from 1.7 to 6.5 and to an inflow Reynolds number Re_1 in the range from 6.3×10^4 to 2.1×10^5 . The inflow Froude number Fr_1 was within 1.54 to 4.95, and from 1.31 to 2.87, for the smooth bed and the pebbled rough bed, respectively.

Table 1. Experimental flow conditions (Present study, $x_1 = 1$ m)

Bed type	h_1 (m)	Q (m ³ /s)	d_1 (m)	Fr_1	Re_1	Comment
smooth	0.03	0.015 to 0.043	0.0315 to 0.0325	1.74-4.95	3.3E+4 to 9.3E+4	High video speed camera, 240fps Point gauge
	0.06	0.036 to 0.095	0.06 to 0.063	1.54-3.93	7.8E+4 to 2.0E+5	
rough	0.06	0.042 to 0.1	0.078 to 0.085	1.31-2.87	9.6E+4 to 2.3E+5	
smooth	0.06	0.078	0.0675	2.84	1.7E+5	Phase-detection dual-tip conductivity probe
rough	0.06	0.06 to 0.1	0.0825 to 0.0835	1.7-2.84	1.4E+5 to 2.2E+5	

To achieve an uniform channel bed roughness, gravels were installed on the whole length of the channel including upstream of and underneath the upstream sluice gate. The same gravel bed was previously used by Li and Chanson (2018). The gravels were fixed on the wooden boards using tile adhesive, (Dunlop, trade resaflex) (Figure 2), Then the boards were installed on the channel HDPE bed from upstream to downstream covering whole length of the channel, including beneath the upstream sluice gate and in the upstream reservoir (Figure 2c). To prevent the uplift of the boards, two plexi-glass walls were fixed to the boards on both sides of flume (Figure 2d). This setup decreased the channel width to 0.475 m. Table 2 lists the properties of gravels. The gravel material was mixed natural river pebbles sieved between 9.5 mm and 13.2 mm, with $d_{50} = 0.011$ m and $\rho_s = 2530$ kg/m³ (Li and Chanson 2018).

Table 2. Properties of gravel

Particle size range (mm)	Weight (g)	Volume (ml)	Density (g/cm ³)	Average density (g/cm ³)
(9.5 to 13.2)	2031.4	800	2.54	2.53
	1920.4	760	2.53	
	1738.4	690	2.52	

3 Basic parameters of hydraulic jump

For all the flow configurations on both smooth and rough beds, free-surface profile recordings were conducted using a pointer gauge. The upstream conjugate depth was measured slightly upstream of the jump toe at $x_1 = 0.9$ m and the subcritical conjugate depth was measured at the downstream end of jump roller. The relationship between conjugate depths ratio and inflow Froude number is presented in Figure 3 for both rough and smooth bed configurations. For rough bed case, Carollo et al. (2009) suggested an empirical relationship between conjugate depths:

$$\frac{d_2}{d_1} = 1 + \sqrt{2} \exp\left(\frac{-K_s}{d_c}\right)(Fr_1 - 1)^{0.963} \quad [1]$$



Figure 1. Initial setup of flume for recording videos with high speed cameras; up: LED light and wall for smooth bed condition and down: LED for rough bed, flow condition: $Q = 0.06218 \text{ m}^3/\text{s}$, $d_1 = 0.082\text{m}$ $Fr_1 = 1.78$, $x_1 = 1\text{m}$ and flow from right to left.

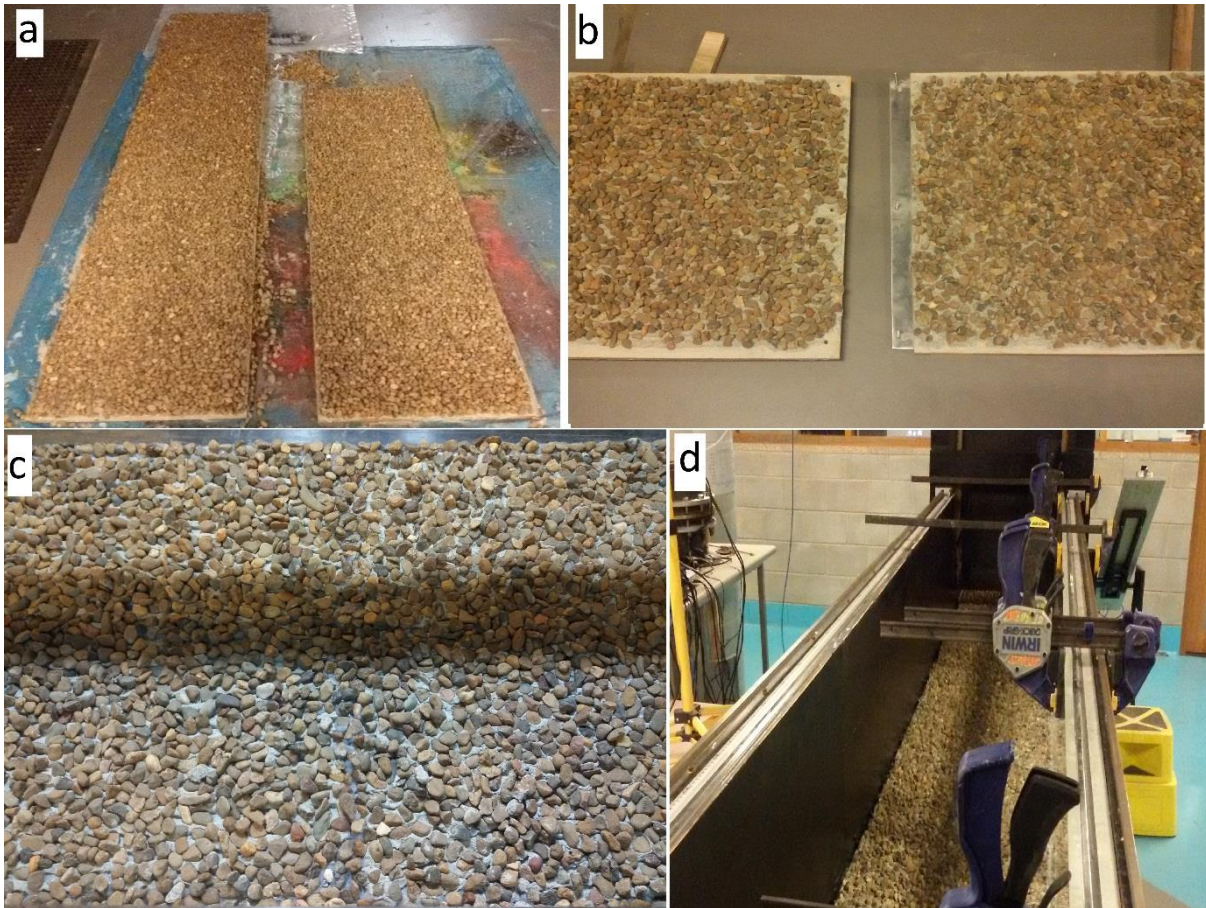


Figure 2. Bed roughness preparation, a: installing gravel, b: attaching plates, c: sticking plates and putting on channel d: black and white walls on two sides

where K_s is the roughness height and equal to d_{50} (the median grain size of sediment particles), and d_c is critical depth of water as $d_c = (q^2/g)^{1/3}$. Considering the present data and those from Felder and Chanson (2016,2018), an empirical relationship was derived herein, relating the conjugate depth ratio with the inflow Froude number Fr_1 and the characteristic roughness (K_s/d_{90}):

$$\frac{d_2}{d_1} = 1 + \sqrt{2} \left(0.7 \exp \left(0.7 \frac{K_s}{d_{90}} \right) (Fr_1 - 1)^{1.05} \right) \quad 1 < Fr_1 < 4 \quad [2]$$

where $K_s = d_{50}$, and d_{90} is the value of grain sizes for which 90% of the material weight is finer. For rough bed data $R^2 = 0.90$ and $SE^2 = 0.35$ while for smooth bed data $R = 0.99$ and $SE = 0.13$. All the present data on both smooth and rough beds were above the dimensionless relationship $d_2/d_1 = Fr_1$, suggested by Ead and Rajaratnam (2002) for hydraulic jumps on corrugated channel beds. The data were in agreement overall with previous studies on roughness effects (e.g. Hughes and Flack 1984; Carollo et al. 2007; Pagliara and Palermo 2015; Felder and Chanson 2018). For $2 < Fr_1 < 2.5$, the conjugate depths ratio for present rough bed as well as roughness type 2 data of Felder and Chanson (2016, 2018) was larger than that based upon the empirical relationship for the rough bed (Eq. 1).

The jump roller length L_r is defined as the longitudinal distance over which the water elevation increases monotonically (Murzyn et al. 2007; Murzyn and Chanson 2009). Herein L_r was derived from the observed mean free-surface profiles. The dimensionless roller length L_r/d_1 is presented in Figure 4 as a function of the inflow Froude number Fr_1 and compared with those from previous studies.

¹ Correlation Coefficient

² Standard Error

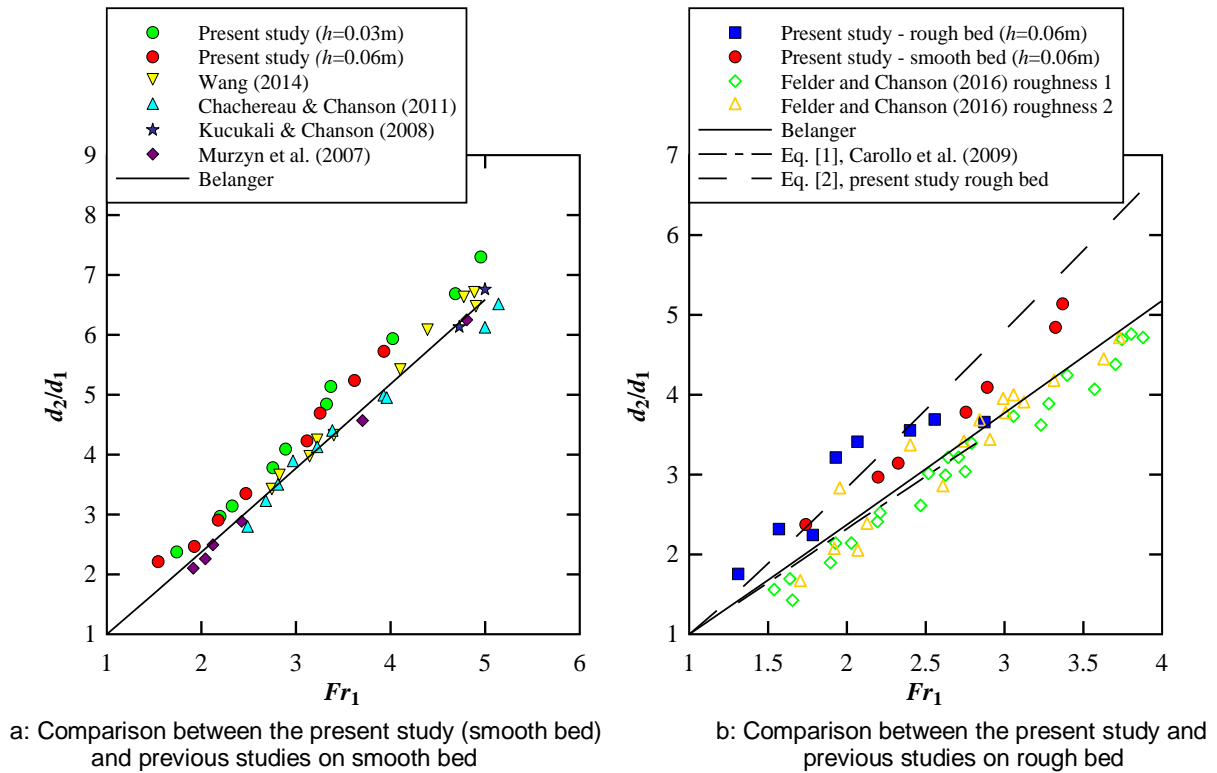


Figure 3. Conjugate depth ratio d_2/d_1

A linear relationship between the relative roller length and inflow Froude number was derived by Wang (2014), and Wang and Chanson (2015) for smooth bed hydraulic jumps:

$$\frac{L_r}{d_1} = 6 \times (Fr_1 - 1) \quad [3]$$

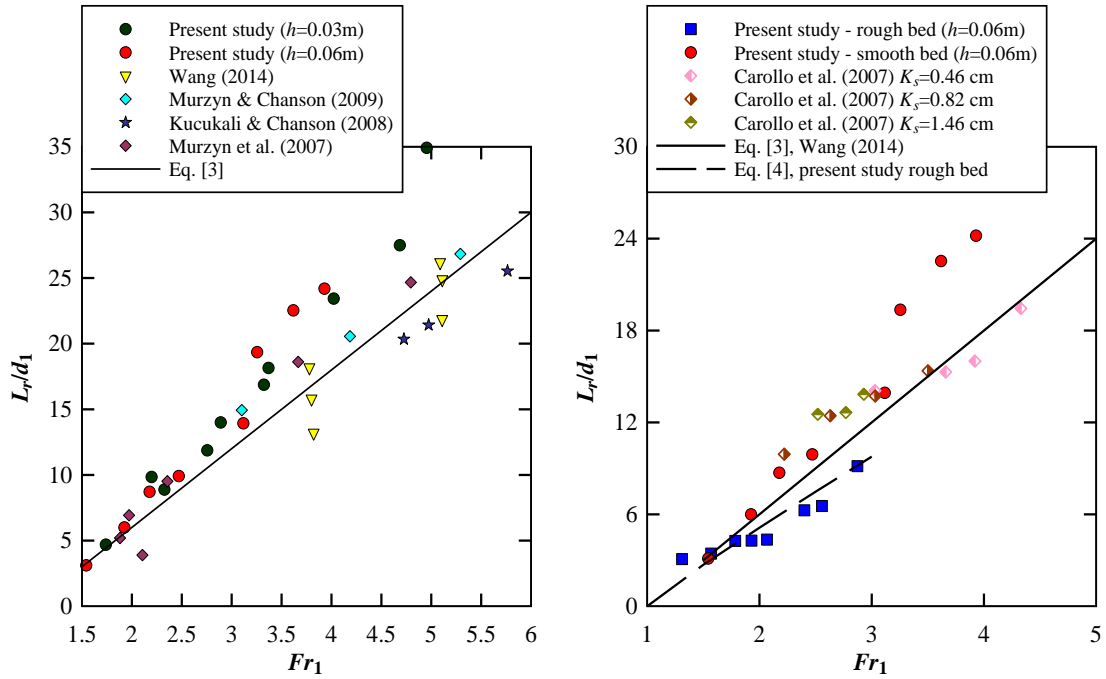
In the present study, an empirical relationship was derived from the present data and those from Carollo et al. (2009) in terms of inflow Froude number and characteristic roughness (K_s/d_1):

$$\frac{L_r}{d_1} = 6 \times (Fr_1 - 1)^{(1 - 0.64 \times \frac{K_s}{d_1})} \quad 1 < Fr_1 < 5 \quad [4]$$

Eq. [4] yielded $R = 0.95$ and $SE = 0.7$ for rough bed condition. In case of $K_s=0$, Eq. [4] led to Eq. [3], i.e. to smooth bed condition, and resulted in $R = 0.98$, and $SE = 1.47$. Figure 4B presents the observed data together with Eqs. [3] and 4. Figure 4b shows that the jump roller length on pebbled rough bed was shorter than that on smooth bed for the same inflow Froude number. It suggested a higher rate of energy dissipation on rough bed. On pebble rough bed, the increase in bed friction led to a shortening of the jump roller length.

4 Air-flow properties

A key air-water flow property is the void fraction C , i.e. the time-averaged air concentration at a position (x, y) within the flow. The time-averaged void fraction C was obtained from the time series of instantaneous void fraction signals recorded by the phase-detection probe. The vertical distribution of void fraction can be approximated by solving the bubble diffusion equation in the turbulent shear layer ($y < y^*$) and free-surface region ($y > y^*$), respectively. In the shear layer, the point source of bubbles is the jump toe, and bubbles are diffused in the vertical direction while advected longitudinally. Thus, the void fraction profile follows a quasi-normal distribution (Chanson 1995, 2010, 2011; Wang and Chanson 2018):



a: Comparison between the present study (smooth bed) and previous studies on smooth bed

b: Comparison between the present study and previous studies on rough bed

Figure 4. Conjugate depth ratio

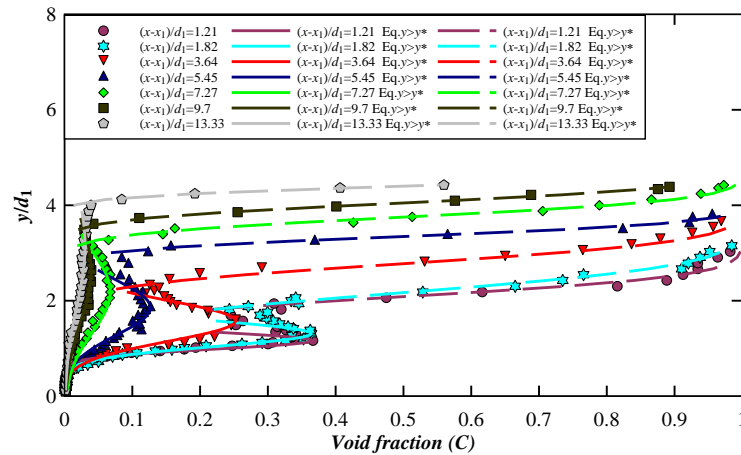
$$C = C_{max} \times \exp \left(- \frac{1}{4 \times D^\#} \times \frac{\left(\frac{y - Y_{C_{max}}}{d_1} \right)^2}{\left(\frac{x - x_1}{d_1} \right)} \right) \quad \text{for } 0 < y < y^* \quad [5]$$

where C_{max} is the local maximum void fraction in the shear layer, $Y_{C_{max}}$ is the vertical position of C_{max} , and $D^\#$ is a depth-averaged diffusivity for $0 < y < y^*$. In the recirculation region, based upon analogy to water jets discharging into air with a uniform velocity distribution suggests that the void fraction follows (Chanson 1989, 2011; Wang and Chanson 2018):

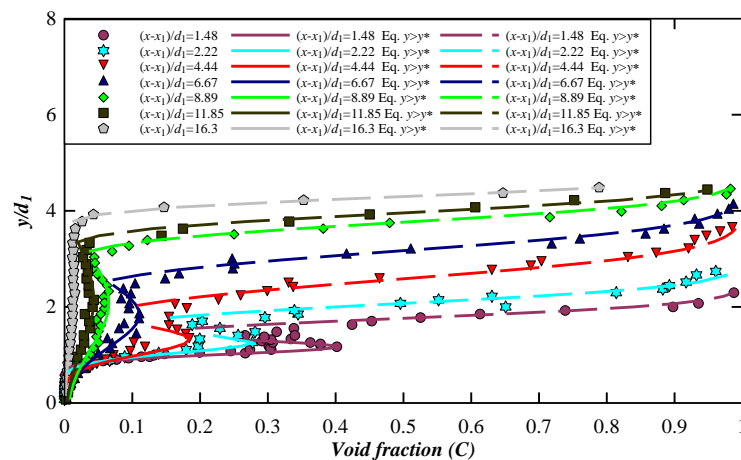
$$C = \frac{1}{2} \times \left(1 + \operatorname{erf} \left(\frac{y - Y_{50}}{2 \times \sqrt{\frac{D^* \times (x - x_1)}{V_1}}} \right) \right) \quad \text{for } y > y^* \quad [6]$$

where Y_{50} is the elevation for $C = 0.5$, D^* is a dimensionless diffusivity in the upper free-surface region, and the Gaussian error function is defined as:

$$\operatorname{erf}(u) = \frac{2}{\sqrt{\pi}} \int_0^u \exp(-t^2) \times dt \quad [7]$$



a: Rough bed, $Q = 0.1 \text{ m}^3/\text{s}$, $d_1 = 0.0825 \text{ m}$, $Fr_1 = 2.84$, $Re_1 = 2.2E+5$



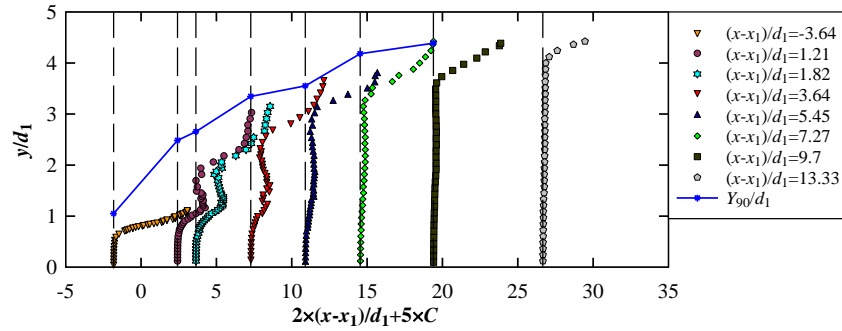
b: Smooth bed, $Q = 0.078 \text{ m}^3/\text{s}$, $d_1 = 0.0675 \text{ m}$, $Fr_1 = 2.84$, $Re_1 = 1.7E+5$

Figure 5. Time-averaged void fraction profiles on the channel centerline, comparison with analytical solution on both rough and smooth beds

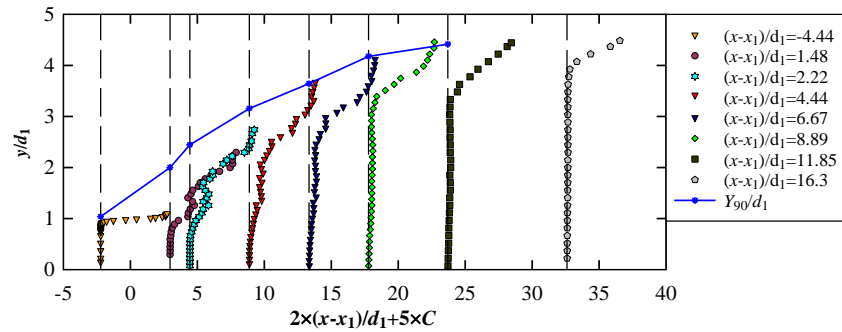
The longitudinal distribution of the vertical profile of the void fraction on both rough and smooth beds with an inflow Froude numbers $Fr_1 = 2.84$ is presented in Figure 5. The data, as well as the visual observations, showed a longer bubbly flow region on rough bed. For $5 < (x-x_1)/d_1 < 9$, the void fraction C in the shear region was slightly higher on rough bed. While for $(x-x_1)/d_1 > 9.0$, on both rough and smooth beds, the void fraction C was almost zero. The comparison of void fraction data between rough and smooth channel beds for the same inflow Froude number $Fr_1 = 2.84$, suggested that the distributions of maximum void fraction C_{max} within the shear layer region were comparable for both configurations: That is, C_{max} was 0.4 and 0.37 at $x-x_1/d_1 = 1.21$ and 1.48 on rough smooth and bed, respectively (Figure. 5 A and D). The dimensionless vertical elevation y/d_1 of local minimum void fraction C^* was higher on the rough bed. Hence close to the jump toe, at first three cross-sections, y_c/d_1 was 1.7, 1.81, 2.17 and 1.41, 1.63, 1.76 on rough and smooth beds, respectively. This resulted in the upward shift of the turbulent shear region with increasing distance from the jump toe on the large bed roughness.

The present findings were in agreement with the results of Felder and Chanson (2016,2018), who compared the air-water flow properties on rough bed (rubber mat roughness) and smooth bed.

The bubble count rate F was linked to the air entrainment and diffusion as well as to the formation, breakup, coalescence and collapse of air bubbles and air pockets in the turbulent shear region. Figure 7 presents typical bubble count rate distributions on both rough and smooth bed configurations. The same upstream aspect ratio $h/W = 0.12$ and inflow length $x_1/h = 16.67$ were used on both rough and smooth bed. In Figure 7, the data shows that the maximum bubble count rate F_{max} in the turbulent shear region was distinctive on both rough and smooth bed configurations and its value decreased with increasing distance from the jump toe. A secondary peak F_{sec} in bubble count rate was observed in the upper flow region. The vertical elevations of the two peak values $Y_{F_{max}}$ and $Y_{F_{sec}}$ increased along the jump roller, together with the increasing free-surface elevation.

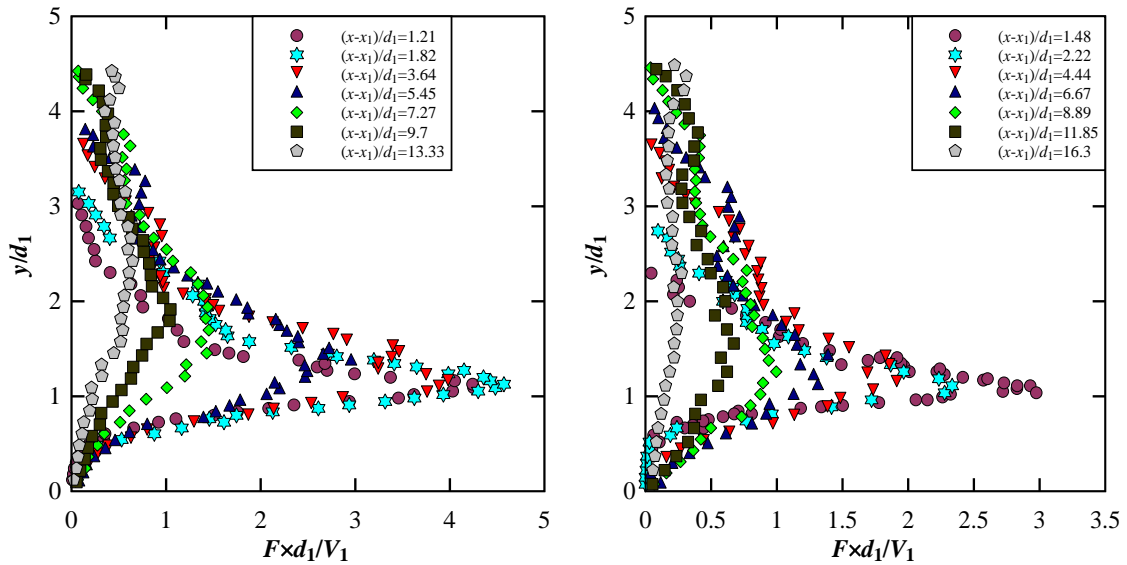


A: Rough bed, Run BR3, $Q = 0.1 \text{ m}^3/\text{s}$, $d_1 = 0.0825 \text{ m}$, $Fr_1 = 2.84$, $Re_1 = 2.2E+5$



B: Smooth bed, Run BS1, $Q = 0.078 \text{ m}^3/\text{s}$, $d_1 = 0.0675 \text{ m}$, $Fr_1 = 2.84$, $Re_1 = 1.7E+5$

Figure 6. Void fraction distributions in hydraulic jump, comparison with the characteristic flow depth Y_{90}/d_1

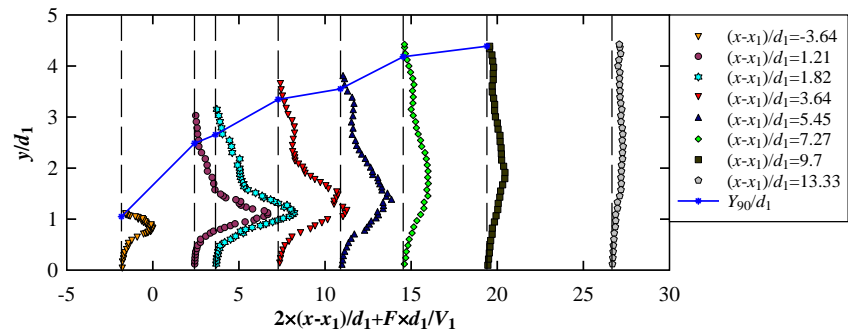


A: Rough bed, Run BR3, $Q = 0.1 \text{ m}^3/\text{s}$,
 $d_1 = 0.0825 \text{ m}$, $Fr_1 = 2.84$, $Re_1 = 2.2E+5$

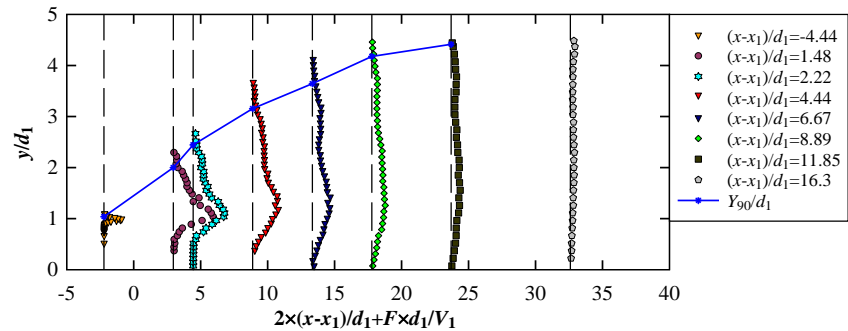
B: Smooth bed, Run BS1, $Q = 0.078 \text{ m}^3/\text{s}$,
 $d_1 = 0.0675 \text{ m}$, $Fr_1 = 2.84$, $Re_1 = 1.7E+5$

Figure 7. Bubble count rate profiles on the channel centerline

The comparison between rough and smooth bed showed higher bubble flux on rough bed configuration, possibly caused by the bed roughness, while the shape of the bubble count rate distributions was the same. For the same Froude number, $Fr_1 = 2.84$, a higher bubble count rate profile was observed at second cross-section $(x-x_1)/d_1 > 1.82$ on rough bed and at first cross-section $(x-x_1)/d_1 > 1.48$ on smooth bed (Figure 7). The longitudinal variation in vertical profiles on both rough and smooth bed configurations with the same inflow Froude number, $Fr_1 = 2.84$, are presented in Figure 8. The characteristic elevation Y_{90} above the invert was added.



A: Rough bed, Run BR3, $Q = 0.1 \text{ m}^3/\text{s}$, $d_1 = 0.0825 \text{ m}$, $Fr_1 = 2.84$, $Re_1 = 2.2E+5$



B: Smooth bed, $Q = 0.078 \text{ m}^3/\text{s}$, $d_1 = 0.0675 \text{ m}$, $Fr_1 = 2.84$, $Re_1 = 1.7E+5$

Figure 8. Bubble count rate distributions in hydraulic jump, comparison with characteristic flow depth Y_{90}/d_1

4 CONCLUSION

The paper presented and discussed basic air-water flow parameters of hydraulic jump, including conjugate depths and jump roller length, on both smooth and pebbled rough bed configurations. The results showed that a larger Froude number Fr_1 resulted in a larger conjugate depths ratio d_2/d_1 and in a longer roller L_r/d_1 with the same trends for both bed types. For the same inflow Froude number, a shorter roller length was observed on rough bed. The basic air-flow properties including void fraction and bubble count rate were also investigated, on both rough and smooth bed configurations. For the same inflow Froude number, the bubbly flow length, as well as the maximum void fraction C_{max} close the jump toe, were larger on rough bed. In the shear region, the larger C^* on rough bed suggested the upward shift of the bubbly flow region on the large bed roughness. In terms of bubble count rate, the vertical elevation of the peak values Y_{Fmax} and Y_{Fsec} increased as the longitudinal distance from the jump toe on both smooth and rough bed increased. A larger bubble count rate was observed on rough bed, possibly caused by the roughness effect.

ACKNOWLEDGEMENTS

The authors acknowledge the technical assistance of Jason Van Der Gevel and Stewart Matthews (Hydraulic Laboratory, The University of Queensland). Farhad Bahmanpouri acknowledges that this research was carried out within his PhD Project and the support from the University of Napoli *Federico II* (PhD Program in Civil Systems Engineering).

REFERENCES

- Carollo, F. G., Ferro, V., and Pampalone, V. (2007). Hydraulic jump on rough beds. *Journal of Hydraulic Engineering*, 133(9), pp. 989–999.
- Carollo, F. G., Ferro, V., and Pampalone, V. (2009). New solutions of classical hydraulic jump. *Journal of Hydraulic Engineering*, 135(6), pp. 527–531.
- Chachereau, Y., and Chanson, H. (2011). Free-Surface fluctuations and turbulence in hydraulic jumps. *Experimental Thermal and Fluid Science*, Vol. 35, No. 6, pp. 896–909 (DOI: 10.1016/j.expthermflusci.2011.01.009).
- Chanson, H. (1989). Study of Air Entrainment and Aeration Devices. *Journal of Hydraulic Research*, IAHR, Vol. 27, No. 3, pp. 301-319 (DOI: 10.1080/00221688909499166).
- Chanson, H. (1995). Air entrainment in two-dimensional turbulent shear flows with partially developed inflow conditions. *International Journal of Multiphase Flow*, Vol. 21, No. 6, pp. 1107-1121 (DOI: 10.1016/0301-9322(95)00048-3).
- Chanson, H. (2004). *The hydraulics of open channel flow: an introduction*. Butterworth-Heinemann, Oxford, UK, 2nd edition, 630 pages.

- Chanson, H. (2009). Advective diffusion of air bubbles in hydraulic jumps with large Froude numbers: an experimental study. *Hydraulic Model Report No. CH75/09*, School of Civil Engineering, The University of Queensland, Brisbane, Australia, 76 pages.
- Chanson, H. (2010). Convective transport of air bubbles in strong hydraulic jumps. *International Journal of Multiphase Flow*, Vol. 36, No. 10, pp. 798-814 (DOI: 10.1016/j.ijmultiphaseflow.2010.05.006).
- Chanson, H. (2011). Hydraulic jumps: turbulence and air bubble entrainment. *Journal La Houille Blanche*, No. 3, pp. 5–16 (DOI: 10.1051/lhb/2011026) (ISSN 0018-6368).
- Ead, S. A., and Rajaratnam, N. (2002). Hydraulic jumps on corrugated beds. *Journal of Hydraulic Engineering*, Vol. 128(7), pp. 656–663.
- Felder, S., and Chanson, H. (2016). An experimental study of air-water flows in hydraulic jumps with channel bed roughness. *WRL Research Report WRL 259*, University of New South Wales, Sydney, Australia, 166 pages (ISBN 9780733436574).
- Felder, S., and Chanson, H. (2018). Air–Water flow patterns of hydraulic jumps on uniform beds macroroughness. *Journal of Hydraulic Engineering*, ASCE, Vol. 144, No. 3, Paper 04017068, 12 pages (DOI: 10.1061/(ASCE)HY.1943-7900.0001402).
- Gualtieri, C., and Chanson, H. (2007). Experimental analysis of Froude number effect on air entrainment in hydraulic jumps. *Environmental Fluid Mechanics*, Vol.7, n.3, June 2007, pp. 217–238.
- Hughes, W. C., and Flack, J. E. (1984). Hydraulic jump properties over a rough bed. *Journal of Hydraulic Engineering* 110 (12), pp. 1755-1771.
- Kucukali, S., and Chanson, H. (2008). Turbulence measurements in hydraulic jumps with partially-developed inflow conditions. *Experimental Thermal and Fluid Science*, Vol. 33, No. 1, pp. 41–53.
- Li, Y., and Chanson, H. (2018). Sediment Motion beneath Surges and Bores. *Proc. 6th IAHR International Symposium on Hydraulic Structures ISHS 2018*, Aachen, Germany, 15-18 May, B.P. Tullis and D.B. Bung Editors, 10 pages (DOI: 10.15142/T3B340).
- Montes, S. J. (1998). *Hydraulics of open channel flow*. ASCE Press, New York, USA, 697 pages.
- Murzyn, F., and Chanson, H. (2009). Experimental investigation of bubbly flow and turbulence in hydraulic jumps. *Environmental Fluid Mechanics*, Vol. 9, No. 2, pp. 143-159 (DOI: 10.1007/s10652-008-9077-4).
- Murzyn, F., Mouaze, D., and Chaplin, J. R. (2007). Air-Water interface dynamic and free surface features in hydraulic jumps. *Journal of Hydraulic Research*, IAHR, Vol. 45, No. 5, pp. 679–685.
- Pagliara, S. and Palermo, M. (2015). Hydraulic jumps on rough and smooth beds: aggregate approach for horizontal and adverse-sloped beds. *Journal of Hydraulic Research*, 53 (2), pp. 243–252.
- Pagliara, S., Roshni, T. and Carnacina, I. (2011). Turbulence, aeration and bubble features of air-water flows over macro- and intermediate roughness. *Water Science and Engineering*, 2011, 4(2), pp. 170-184, DOI: 10.3882/j.issn.16742370.2011.02.005.
- Rajaratnam, N. (1967). *Hydraulic jumps*. *Advances in Hydroscience*, Vol. 4, Ed. by V. T. Chow, Academic Press, N.Y., pp. 197-280.
- Rao, N. S. L., and Kobus, H. E. (1971). *Characteristics of self-aerated free-surface flows*. Water and Waste Water/Current Research and Practice, Vol. 10, Eric Schmidt Verlag, Berlin, Germany.
- Valero, D., Viti, N., and Gualtieri, C. (2019). Numerical simulation of hydraulic jumps. Part 1: Experimental results for performance assessment. *Water*, 2019, 11(1), January 2019, 36, DOI: 10.3390/w11010036.
- Wang, H. (2014). Turbulence and air entrainment in hydraulic jumps. *Ph.D. thesis*, School of Civil Engineering, The University of Queensland, Brisbane, Australia (DOI: 10.14264/uql.2014.542).
- Wang, H., and Chanson, H. (2015). Air entrainment and turbulent fluctuations in hydraulic jumps. *Urban Water Journal*, Vol. 12, No. 6, pp. 502–518 (DOI: 10.1080/1573062X.2013.847464).
- Wang, H., and Chanson, H. (2016). Self-Similarity and scale effects in physical modelling of hydraulic jump roller dynamics, air entrainment and turbulent scales. *Environmental Fluid Mechanics*, Vol. 16, pp. 1087–1110 (DOI: 10.1007/s10652-016-9466-z).
- Wand, H., and Chanson, H. (2018). Estimate of void fraction and air entrainment flux in hydraulic jump using Froude number. *Canadian Journal of Civil Engineering*, Vol. 45, No. 2, pp. 105-116 (DOI: 10.1139/cjce-2016-0279).
- Wood, I. R. (1991). *Air entrainment in free-surface flows*. IAHR Hydraulic Structures Design Manual No. 4, Hydraulic Design Considerations, Balkema Publisher, Rotterdam, the Netherlands, 149 pages.